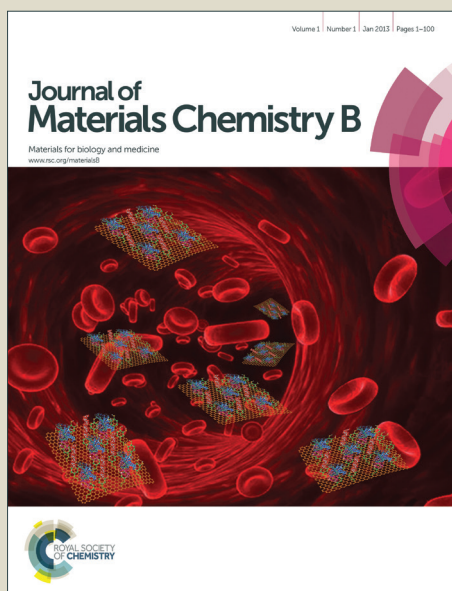


Journal of Materials Chemistry B

Accepted Manuscript



This is an *Accepted Manuscript*, which has been through the Royal Society of Chemistry peer review process and has been accepted for publication.

Accepted Manuscripts are published online shortly after acceptance, before technical editing, formatting and proof reading. Using this free service, authors can make their results available to the community, in citable form, before we publish the edited article. We will replace this *Accepted Manuscript* with the edited and formatted *Advance Article* as soon as it is available.

You can find more information about *Accepted Manuscripts* in the [Information for Authors](#).

Please note that technical editing may introduce minor changes to the text and/or graphics, which may alter content. The journal's standard [Terms & Conditions](#) and the [Ethical guidelines](#) still apply. In no event shall the Royal Society of Chemistry be held responsible for any errors or omissions in this *Accepted Manuscript* or any consequences arising from the use of any information it contains.

ARTICLE

A paper based, all organic, reference-electrode-free ion sensing platform

Cite this: DOI: 10.1039/x0xx00000x

Johannes Kofler^a, Sebastian Nau^a and Emil J. W. List-Kratochvil^{a,b},

Received 00th January 2012,
Accepted 00th January 2012

DOI: 10.1039/x0xx00000x

www.rsc.org/

We present a reference-electrode free, all organic K⁺ sensitive ion sensing platform fabricated by simplest means on a plain sheet of paper. This platform is based on two identical ion selective electrodes (ISEs) which are assembled by bonding a polymeric ion selective membrane (ISM) directly onto a drop-casted PEDOT:PSS electrode. Taking full advantage of the so called pulsetrode concept, a current pulse is used to measure the concentration of the targeted ion. The current forces an ion flux out of the first ISE, through the sample and into the second ISE. This flux leads to a well-defined potential jump at the second ISE, as soon as the target ion locally depletes within the analyte, whereas the current induced potential change at the first ISE does not depend noticeably on the type of background electrolyte. Hence, the potential difference between the ISEs, required to apply the current is directly related to the ion concentration within the sample. This concept allows for a 20-fold sensitivity enhancement compared to classical potentiometric measurements in physiological backgrounds. As mutual potential drifts of the ISEs cancel out, the sensor response showed excellent stability and did not change during multiple measurements over three months.

Introduction

Ion sensors are required in many fields ranging from food safety control¹, water quality monitoring²⁻⁴ to various applications in pharmaceutical and cosmetics industry.⁵ Especially within the emerging fields of clinic analysis low-cost sensor platforms for in-situ sensing of ions and biological substances in appropriate aqueous media and physiological backgrounds are required.⁶ Potentiometric ion-selective electrodes (ISEs) are established tools as a routine methodology in clinical diagnostics for the determination of small hydrophilic target ions.⁷ In particular ISEs based on polymeric ion selective membranes (ISMs) containing neutral or charged carriers (ionophores) have been improved to such an extent that it has resulted in a “new wave of ion-selective electrodes”.^{7,8} This was achieved by considerable improvements of the lower detection limit, new membrane materials, and a deeper theoretical understanding of the potentiometric response of ISMs. The discovery of transmembrane fluxes and the fact that leaking of target ions into the sample reduces the lower detection limit, revolutionized the field.^{9,10} Today, ISEs with extremely high selectivity⁸ and detection limits down to low nano-molar levels are available.¹¹⁻¹⁴ Recently, low cost organic potentiometric sensors have emerged.^{15,16} The sensitivity of all of these electrodes is typically given through the Nernst equation limiting it to ~59 mV for a 10 fold sample activity change in case of a monovalent ion. A second important

limitation of ISEs is that in order to reliably measure the electromotive force (EMF) and to obtain a stable sensing signal, at least one reference electrode is required. However, the bridge electrolyte and the liquid junction of classical reference electrodes require regular maintenance, a vertical working position, and it may also contaminate the sample. Although promising liquid junction-free all solid state reference electrode concepts were demonstrated¹⁷⁻²³, the potential stability upon varying the ionic strength²⁴ and response time of these novel solid-state reference electrodes still bear challenges.

Typically ISEs are operated potentiometrically in chemical equilibrium. However, recently various attractive non-equilibrium current and potential techniques have emerged.⁵ These techniques can overcome the limits of conventional ISEs. In particular flash chronopotentiometry (pulsetrodes), which allows for 10 to 20-fold sensitivity enhancement compared to classical potentiometry, seems to be especially suited for ion sensing in physiological backgrounds.²⁵⁻²⁷ The pulsetrode principle is based on a constant current pulse which forces a ion flux into the ISM. This constant ion flux leads to a local depletion of the target ion in the analyte which is accompanied by a drastic potential change (potential jump) at a certain transition time. Hence, the potential recorded at a fixed pulse time is a function of the labile ion concentration within the analyte^{5,26} and exhibits a very high sensitivity within a narrow concentration range.²⁶ After each measurement the ISM has to be regenerated by applying the initial equilibrium potential

measured before the current pulse is applied.²⁵ For that reason, reference electrodes are still necessary.

The aim of this work is to present a flash-chronopotentiometric, all organic and reference electrode free K^+ sensing platform on paper. This platform is based on two identical PEDOT:PSS-based solid contact ISEs (SC-ISEs) fabricated on a paper sheet by simplest means (see figure 1a). The novelty of the proposed measurement method is that the commonly used reference electrode is replaced by a second, identical ISE. To measure the concentration of the target ion a constant current pulse is forced through the ISEs while the potential difference between the ISEs is measured at a fixed measurement time t_{meas} (see figure 1b, V_{SENS}). The current forces an ion flux through the sample and through both ISEs. The ISE operated in forward direction (ISE_{IN}), extracting target ions into the membrane from the sample side, will exhibit the typical potential jump upon target ion depletion (see figure 1b V_{IN} and figure 1c). The ISE operated in backward direction (ISE_{OUT}) just shifts the potential difference between the ISEs by a constant value, and thus does not disturb the measurement signal (see figure 1b V_{OUT}). Since both ISEs are identical, the equilibrium potentials of both ISEs are equal with respect to the analyte and the ISEs can be regenerated simply by shortening them after each measurement. Consequently, the second ISE serves two purposes. Firstly, it provides a reference potential during the measurement pulse

and secondly it allows to regenerate the ISEs without using a reference electrode. Additionally, mutual potential drifts of the ISEs cancel out, leading to a very stable and reproducible response.

To generalize the proposed sensing method and to demonstrate that the sensing signal solely arises at the ISM-sample interface, two conventional ISEs, containing aqueous inner filling solutions, were used in a first step. The results were modelled by numerical calculations, gaining insight into the response mechanisms and revealing the limits of the measurement-parameters, namely the maximum pulse time. In a second step, the response of the all organic PEDOT:PSS-based SC-ISEs is investigated. The SC-ISEs exhibit the same characteristics as the conventional setup. In accordance with the results reported by S. Makarychev-Mikhailov et al.²⁷, a 20-fold sensitivity enhancement compared to classical potentiometric measurement was obtained. Therefore, the sensing platform and the measurement method presented within this work perform comparable to other flash-chronopotentiometric devices. Importantly, this platform does not require a reference electrode, it is all-organic and very simple to fabricate. Furthermore, stability measurements reveal that the response signal was stable for at least 3 months.

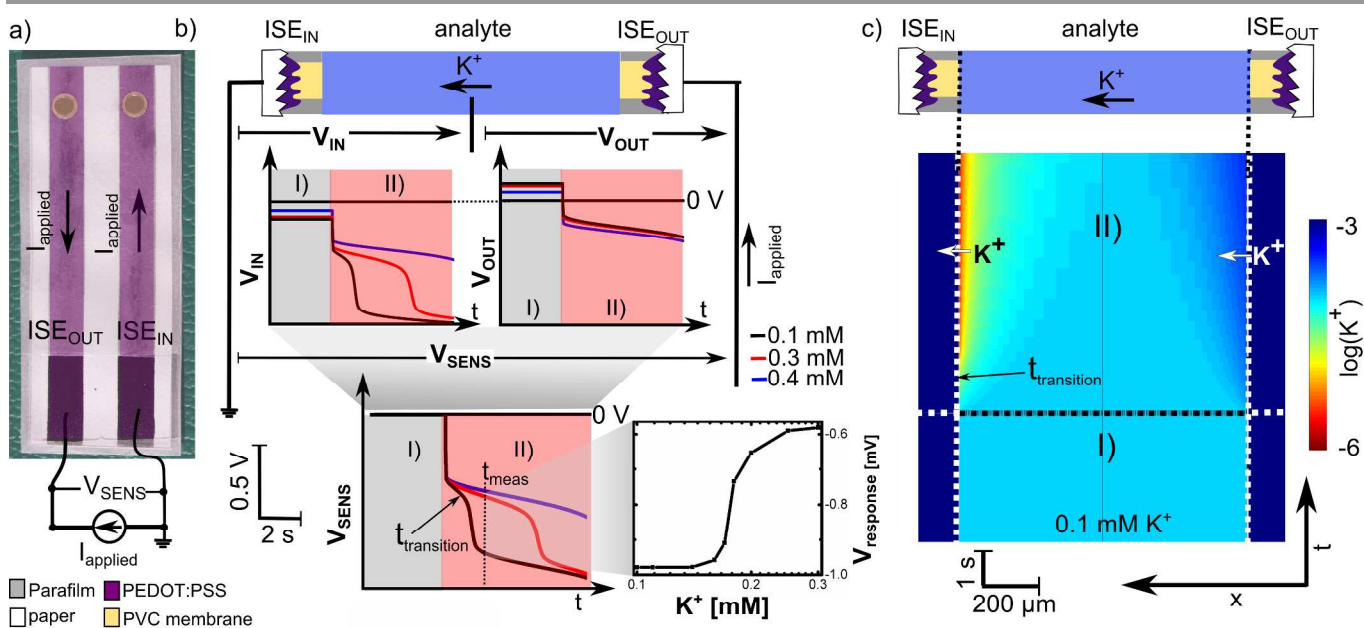


Figure 1: a) An image of a fabricated sensor and its circuit diagram (the materials are additionally dyed for a better understanding); b) Illustration of the sensing principle: A measurement cycle consists of a regeneration (I, both ISEs are shortened) a constant current measurement pulse (II) and an inverse regeneration pulse (III, not shown). The membrane potentials of ISE_{IN} (V_{IN}), ISE_{OUT} (V_{OUT}) and the potential difference between the ISEs (V_{SENS}) during a measurement cycle at different K^+ concentrations (0.1 mM black, 0.3 mM red, 0.4 mM blue), is shown on the top left, top right and left bottom. To measure the concentration a constant current pulse is applied (I_{applied}) while the potential V_{SENS} is recorded at a fixed time t_{meas} . The accordingly measured response (V_{response}) is shown on the bottom right; c) the numerically calculated K^+ concentration during a measurement cycle (bulk analyte concentration 0.1 mM K^+).

Theory

Generally, chronopotentiometric measurements are based on ion transfer at immiscible electrolyte solutions (ISM, aqueous

analyte).⁵ For that reason, to describe the response of a chronopotentiometrically operated ISM, all transferring ions within the analyte and the ISM have to be considered. Highly ion selective plasticized PVC membranes contain an ionophore

(L), anionic sides (R^-) and a background electrolyte (B^+/B^-) (see figure 2a). These anionic sides fix the concentration of ionophore-target ion concentration (LK^+) and the background electrolyte ensures a high conductivity of the membrane.⁵ However, the sensing mechanism is chemically based on the recognition of an aqueous target ion by an ionophore, which thermodynamically facilitates selective ion transfer (IT) into the membrane. The strong ion - ionophore interaction overcomes the unfavorable free energy of transfer and hydrophilic ions are extracted into the hydrophobic membrane developing a Nernstian phase boundary potential in equilibrium²⁸. The Nernstian phase boundary potential is used as a measurement signal for potentiometric measurements, limiting the response to a sensitivity of ~ 59 mV per 10 fold activity change in case of a monovalent ion. Upon applying a constant current pulse, ions are forced into the membrane on the front side of ISE_{IN} and out of the membrane on the back side of ISE_{OUT} . As the transfer of the target ion (K^+) into the membrane is facilitated by the ionophore, exclusively K^+ ions are extracted into ISE_{IN} . Likewise, K^+ ions are extracted into the analyte at ISE_{OUT} (mechanism 1' in figure 2b). At the beginning of the pulse, as long as the ion concentrations at the interface are proportional to the bulk ion concentrations, the response obeys a near-Nernstian slope towards the respective activity (see also SUI S2).^{29,30} At larger pulse times, the target ion is depleted. The square route of the time when the target ion depletes (transition time) is linearly proportional to the concentration and inversely proportional the current density. As soon as the target ion depletes within the sample, other positively charged ions have to be transferred into the membrane or negatively charged ions within the membrane have to be extracted into the analyte (see mechanism 2' in figure 2). As the free energy of transfer of these ions is higher, a larger potential has to be applied to keep the ion flux through the ISM-analyte interface constant. The magnitude of this potential change (potential jump) is directly related to the selectivity of the membrane; i.e. to the difference of the free energy of transfer between the target ion and the alternatively included/extracted ion. However, similar depletion effects can also occur within the membrane. The freely available ionophores (L) at ISE_{IN} or the complexed target ions (LK^+) at ISE_{OUT} can deplete earlier than the target ion. Likewise, alternative ions are extracted into the analyte or the membrane (see figure 2b, mechanisms 3' and 4').

There are analytical and numerical models which describe the chronopotentiometric operation of an ISM.^{29,31-35} These models only consider ion transfers of target and interfering ions and they neglect the influence of the electric potential. In contrast, the numerical calculations presented here, take all transferring ions as well as the electric potential, into account. A detailed description of the method can be found in the SUI (S1). Briefly, similar to the method described in ref.³⁶ and ref.³¹ the system was separated into three layers (analyte, ISM, inner filling solution). The bulk of these layers were calculated by solving the Nernst Planck and Poisson differential equations (NPP) as described in ref.³¹. The mass transport of a specific ion in between the layers and thus through interfaces were modelled

using the Butler-Volmer-type relations which describe the transfer rates as a function of the potential drop at the interface.²⁸

Experimental

Chemicals and Materials

The ISM contained the cation exchanger sodium tetrakis[3,5-bis(trifluoromethyl)phenyl]borate (NaTFPB) (15 mM/kg), the potassium ionophore I (valinomycin, 5 mM/kg) and the background electrolyte tetradodecylammonium (TDA) tetrakis(4-chlorophenyl)borate (TCIPB) (ETH 500, 20 mM/kg). The membrane matrix contained high molecular weight polyvinyl chloride (33 wt%, Selectophore grade) and the plastisizer 2-nitrophenyl octyl ether (2-NPOE) (67 wt%). The ISM cocktails were dissolved in tetrahydrofuran (THF) and drop casted onto a confined glass sheet. The drop-cast membrane was allowed to dry overnight at ambient conditions in a saturated THF environment and was peeled off for further implementation. The final thickness of the ISM was ~ 150 μm . All of the chemicals mentioned above were obtained from Fluka Sigma- Aldrich and were used as received. The saline solutions were prepared with KCl ($>99.0\%$), CaCl_2 ($>99.0\%$), Na_2SO_4 ($>99.0\%$), citric acid ($>99.0\%$) and deionized water.

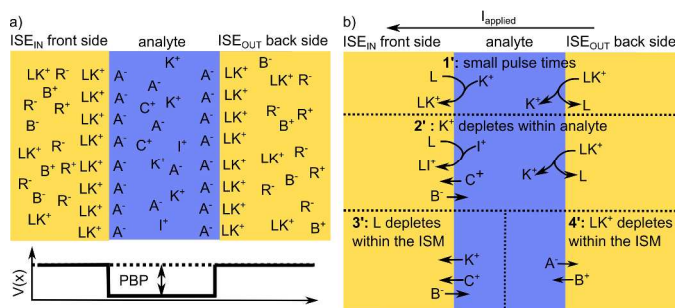


Figure 2: a) Illustration of the ions present within the membrane/analyte and the formation of the Nernstian phase boundary potential (PBP) in equilibrium. K^+ corresponds to the target ion, I^+ to the interfering ions, C^+/A^- to background cations/anions in the analyte, R^- to anionic sides in the ISM and B^+/B^- to background cations/anions in the ISM, L is the freely available ionophore and LK^+/LI^+ is the ionophore- K^+/L^+ complex; b) illustrations of possible mechanisms occurring at the front side and backside of an ISM during a constant current pulse (for further details see text).

Sensor fabrication

First, the design of the PEDOT:PSS electrodes was printed in black & white on a copy-paper (copy paper "Blustar" 80 g/m²). The PEDOT:PSS electrodes are simply structured by drop casting PEDOT:PSS (CleviosTM PH 1000) onto these printed electrodes. As the inkjet printing paper is initially hydrophobic and the water based ink hydrophilic, PEDOT:PSS is confined to the hydrophilic printed areas. After drop casting PEDOT:PSS, the paper is transferred into an oven and dried for 1 h at 150 °C. The resistance of the PEDOT:PSS electrodes (1 cm wide and 5

cm long) is in the range of 30 k Ω . Subsequently, the paper is made water impermeable by laminating a Parafilm M[®] at $\sim 100^{\circ}\text{C}$ onto the top and the bottom side of the paper. Prior to lamination two holes (2 mm and 3 mm diameter), which accommodate the ISMs, were punched into the Parafilm M[®] using a biopsy punch. The ISMs are cut out of a bigger ISM sheet using a biopsy punch with a diameter of 4 mm. The sensor is finalized by gluing these ISMs onto the PEDOT:PSS electrodes. This is done by drop-casting 5 μL THF onto the ISM and immediately thereafter placing the ISM with the THF side first onto the PEDOT:PSS electrodes. THF partly dissolves the ISM leading to a conformal contact between the ISM and the PEDOT:PSS electrodes and to a tight sealing at the ISM edges. After gluing, the sensor is left to rest for ~ 12 h in order to let the residual THF evaporate. After fabrication, the sensors were conditioned for ~ 5 h in a 1 mM KCl solution to exchange the Na^+ ions of the NaTFPB within the membrane with the targeted K^+ ions. After the conditioning the sensors were blow dried and subsequently stored in dark under ambient conditions until measurement. Note that the ISEs were spaced 5 mm apart in order to avoid cross talk.

Measurement setups/procedures

Current and potentials were measured using a B1500A Parameter analyzer. To carry out potential measurements, the source-measurement units were operated as 0 A constant current sources while measuring the potential. To apply a current pulse, the current was set to the corresponding value and the potential was measured. To carry out the reference measurements (conventional setup) two custom made ISEs were used. The inner filling solutions (IFS) (10 mM KCl in a 10 mM CaCl_2 background) of the ISEs were contacted with Ag/AgCl reference electrodes whereas the PEDOT:PSS based solid state ISEs were contacted by two alligator clamps. In order to investigate the ISEs separately, an additional reference electrode contacting the analyte, was used. The reference electrode was placed half way between the ISEs. A measurement cycle was carried out as follows. First, a base line potential-pulse is applied (0 V to both ISE terminals) while the current flowing between the ISEs is monitored. This current should ideally be 0 A in equilibrium. This base line pulse was applied for 6 min in between the current pulses. Subsequently, a current pulse and a reverse regeneration pulse was applied and the potential was monitored at all three reference electrodes. No working electrodes were used and the currents applied during the measurement cycles were passing through the reference electrodes contacting the IFS. The recorded potentials are therefore biased by a current induced potential drop at the reference electrodes. However, these potentials drops are constant and therefore solely result in a constant offset which does not influence the measurement signal as such. Furthermore note that all measurements were carried out using excess background electrolytes to avoid migration effects within the analyte.

Results and discussion

First, to generalize the measurement method, two conventional ISEs containing an aqueous inner filling solutions (liquid contact), were used. Liquid contacts are well-defined systems which can be described numerically. Hence, it is possible to identify the mechanisms and the operational limits of the sensor. Furthermore, it is verified that the sensing signal solely arises at the ISM-sample interface and not at the PEDOT:PSS solid contact, implying the possibility to use this measurement method for various other ISEs. In the thereafter following step, the PEDOT:PSS-paper based SC-ISEs are characterized and the sensitivity and long term stability of the sensing platform is demonstrated.

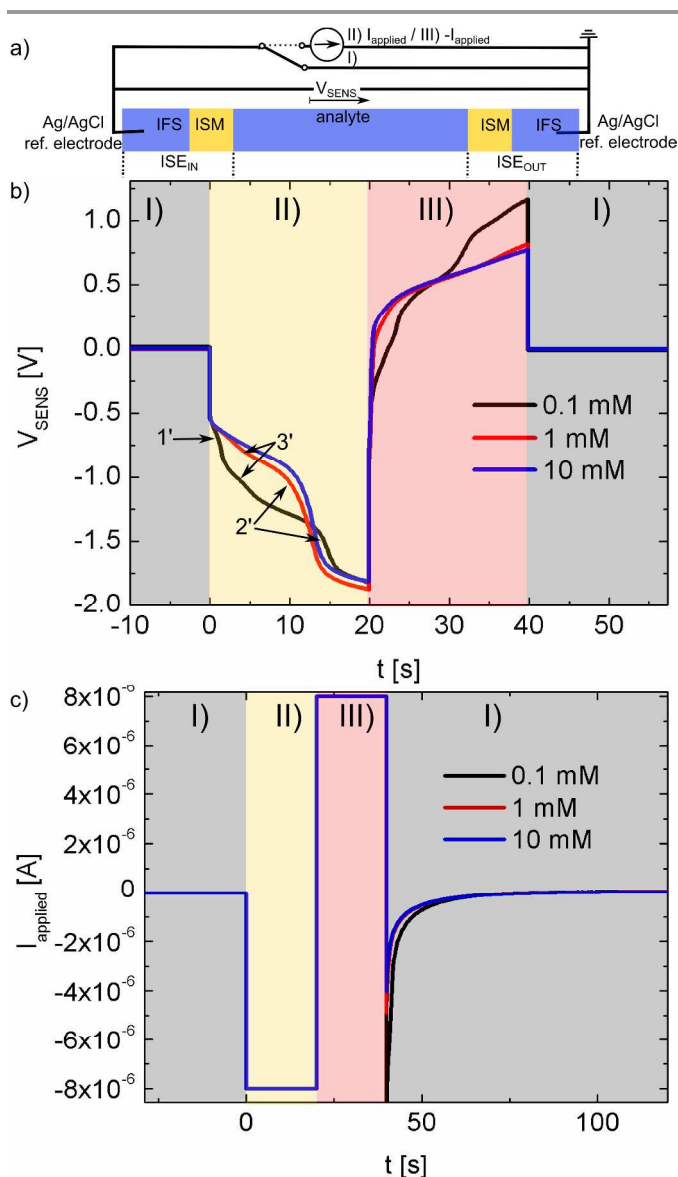


Figure 3: a) Simplified circuit diagram of the measurement setup showing two ISEs with identical inner filling solutions (IFS) which are operated in series. In between the measurements, the ISMs are regenerated by applying 0 V to both ISEs. This is equivalent to a shorting, which is illustrated by a switch in position I); during the measurement pulse and the reverse pulse the switch is in position II) or III) respectively; b) sensing signal (V_{SENS}) measured in analytes at

concentrations of 0.1 mM (black), 1 mM (red), 10 mM KCl (blue) in an 10 mM CaCl_2 background during a full measurement cycle consisting of a regeneration (grey region I), a measurement pulse (yellow region II) and an inverse pulse (red region III). The observable transition times are marked with numbers 1'-3'. The applied current density was $\sim 0.4 \mu\text{A}/\text{cm}^2$. The corresponding currents are shown in c).

Conventional setup

The response curves and the applied currents at concentrations of 0.01, 1, 10 mM KCl in a 10 mM CaCl_2 M background of a measurement setup using two conventional ISEs are shown in figure 3. First, both ISEs are forced to 0 V which is equivalent to shortening both ISEs (see region I in figure 3). As both ISEs are identical they ideally have the same equilibrium potentials with respect to the analyte. Consequently, only a negligible faradaic current is flowing in between the ISEs (see figure 3b region I). After an equilibration time of 5 minutes, a current is applied to the ISEs, forcing K^+ ions from the analyte into the membrane on one side and vice versa on the other side (see region II in figure 3). The potential difference in between the ISEs corresponds to the measurement response which strongly depends on the target ion concentration within the analyte. After this first current pulse a second inverse pulse, with identical but negative current, is applied. This leads to a faster regeneration of the membrane²⁵ (region III). After the measurement, both ISEs are forced to 0 V to regenerate the ISEs. During the regeneration, the current flowing between the ISEs decreases until it eventually reaches a very small steady state current ($\sim 0.7 \text{ nA}/\text{mm}^2$). The remaining steady state current can be attributed to a small potential difference between the reference electrodes, non-idealities of the membranes or to the measurement setup itself (potential differences as small as $\sim 0.4 \text{ mV}$ are sufficient to explain this current). However, currents of these small magnitudes are not sufficient to perturb the ISM and the thereafter following measurements at concentrations examined within this work.

There are three different potential jumps observable in figure 3b. In order to ensure that the sensing signal solely depends on the target ion concentration and not on the type of background anion, it is crucial to identify the origins of the potential jumps. For that reason each ISE was investigated separately in various background electrolytes by monitoring the potential of the analyte with an Ag/AgCl reference electrode.

The experimentally measured as well as numerically calculated response curves of ISE_{IN} at concentrations of 0.1, 1, 10 mM KCl in an 10 mM CaCl_2 , a highly interfering 10 mM NaCl and 5 mM Na_2SO_4 background are shown in figure 4 a. These two background cations represent two extremes; Ca^{2+} is very hydrophilic and non-interfering ion, whereas Na^+ is one of the major interfering ions (in case of the valinomycin ionophore).

At the end of the regeneration, the membrane potential depends on the concentration within the electrolyte in a Nernstian fashion (56 mV per 10 fold activity change, see figure 4, region I). Likewise at the beginning of the current pulse the membrane potential exhibits a near Nernstian response towards the

respective activities of the target ion, as long as no concentration polarization occurs (refer to SUI S2 for details). As two ISEs are operated in series, Nernstian responses cancel out in the final response curve. Hence, as long as no concentration polarization occurs, the total response of the sensor does not depend on the concentration of the targeted ion. The first potential jump is observed at a concentration of 0.1 mM K^+ in a CaCl_2 electrolyte (point 1'). In case of the NaCl electrolyte the magnitude of this potential jump is not as pronounced and a second potential inflection is observed at larger pulse times (point 2*). At K^+ concentrations of 1 mM and 10 mM one potential jump is observed in both background electrolytes (point 2').

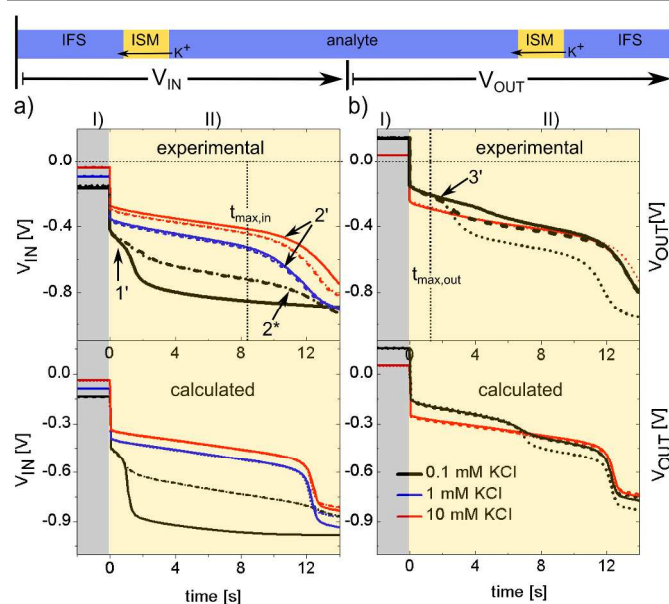


Figure 4: Measured (top) and numerically calculated response (bottom) of ISE_{IN} (a) and ISE_{OUT} (b) during a measurement cycle at concentrations of 0.1 mM, 1 mM and 10 mM KCl in a 10 mM CaCl_2 (solid lines), a 10 mM NaCl (dashed lines) and a 5 mM Na_2SO_4 background (dotted lines). For reasons of clarity, the response at 1 mM KCl was omitted in b). Furthermore note that the curves at concentrations of 1 mM and 10 mM KCl of the different background electrolytes largely overlap. The characteristic transition times are marked with numbers (for details see text). The maximum applicable pulse times ($t_{\text{max,out}}$, $t_{\text{max,in}}$) are marked by a vertical lines. The applied current density was $\sim 0.4 \mu\text{A}/\text{mm}^2$.

Evidently, the numerical solutions of the NNP equations agree qualitatively with the response curves obtained. The concentration profiles of the charged species are shown in the SUI (S3). According to the numerical solutions of the NNP equations, the potential inflection in point 1' is due to the depletion of the target ion within the aqueous sample. The square root of the transition time of this potential jump is proportional the labile ion concentration of the targeted K^+ ion and is responsible for the sensing signal. In case of the NaCl background, interfering Na^+ ions can easily be extracted into the membrane as soon as the K^+ ion depletes within the aqueous layer. Whereas in case of the CaCl_2 background, due to the high hydrophilicity of Ca^{2+} (high free energy of transfer from the aqueous analyte into the hydrophobic ISM), primarily TCIPB^- ions (background electrolyte of the membrane) are forced from

the membrane into the water. The extraction of TCIPB^- requires a higher potential than the assisted ion transfer of Na^+ . This is the reason why the magnitude of the potential jump is lower in case of the highly interfering NaCl background. The second inflection in point 2* can be ascribed to ionophore depletion within the membrane. As soon as the freely available ionophores deplete at the membrane surface, the assisted ion transfer gets halted. As Na^+ is very hydrophilic, primarily TCIPB^- ions are extracted from the membrane into the water. The same mechanism is also responsible for the potential inflection at point 2'. At high K^+ concentrations (1 mM and 10 mM) the freely available ionophore depletes, leading to a potential inflection which is identical to the one observed at point 2*. Hence, this potential jump does not depend on the labile concentration of K^+ and can therefore not be used as a sensing signal.

The experimental (top) as well as the numerically calculated response curves (bottom) of ISE_{OUT} are shown in figure 4 b. This time the anion is drawn towards the membrane. This is why an alternative anion was studied. SO_4^{2-} is extremely hydrophilic (on the right in the Hoffmeister series) and will therefore require a significant higher potential to be extracted into the membrane than Cl^- . As in the case of ISE_{IN} , at the beginning of the current pulse (< 2 s) the response is near Nernstian cancelling itself out in the final response curve. At higher pulse times and low K^+ concentrations of 0.1 mM, two inflection points are observable. According to the numerical solutions of the NPP equations, the potential jump 2' can again be ascribed to ionophore depletion and is identical to the one observed at 10 mM K^+ at ISE_{IN} . Thus, the K^+ ions within the inner filling solution deplete the ionophore on the inner filling solution side. The potential jump 3', can be ascribed to a depletion of complexed LK^+ on the sample side. As soon as LK^+ depletes, anions from the sample are extracted into the membrane. As SO_4^{2-} has a higher free energy of transfer and is found to the right of Cl^- in the Hoffmeister series, a more prominent backside depletion is observable.

To summarize, the measurement response only depends explicitly on the K^+ concentration within the analyte as long as no LK^+ depletion occurs at ISE_{OUT} . As soon as LK^+ depletes on the sample side at ISE_{OUT} , anions have to be extracted from the sample into the membrane leading to a potential jump. The magnitude of this potential jump and therefore also the sensor response depends on the type of transferring anions present in the analyte. For that reason, in order to avoid a mixed signal from the anion and the targeted K^+ ion, the maximum applicable pulse time is limited to $t_{\text{max,out}}$ (see vertical dotted line in figure 5 b). LK^+ depletion can be avoided if the current density through ISE_{OUT} is smaller than through ISE_{IN} . Thus, the surface area of ISE_{OUT} has to be larger than of ISE_{IN} . However, ionophore depletion at the sample side of ISE_{IN} leads to a selectivity breakdown giving rise to the upper detection limit ($t_{\text{max,in}}$ see vertical dotted line in figure 4 a). The response at concentrations exceeding this upper detection limit and concomitant higher pulse times, is only determined by the

concentration and diffusion of freely available ionophore within the membrane.

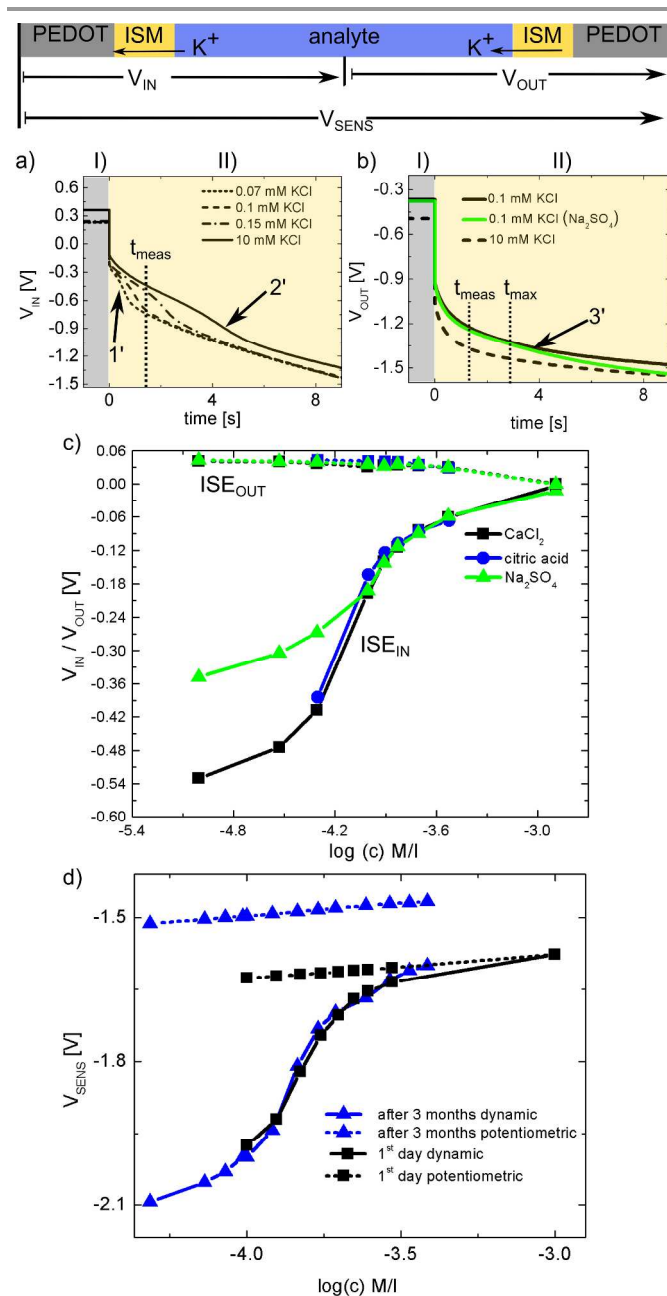


Figure 5: a) response of the SC-ISE operated in forward direction (ISE_{IN}) in a 10 mM CaCl_2 background at different KCl concentrations. b) response of the ISE operated in backward direction (ISE_{OUT}) in a 10 mM Na_2SO_4 background and a 10 mM CaCl_2 background at a KCl concentrations of 0.1 mM and 10 mM. The observable transition times are marked with numbers (for details please refer to text); The sensor was driven at a current density of $\sim 0.6 \mu\text{A}/\text{mm}^2$ (ISE_{IN}) and $\sim 0.4 \mu\text{A}/\text{mm}^2$ (ISE_{OUT}); c) The response of ISE_{IN} (solid lines) and ISE_{OUT} (dotted lines) in a 10 mM CaCl_2 , a 10 mM Na_2SO_4 and a 10 mM citric acid background recorded at t_{meas} (1.8 s). The response of ISE_{IN} and ISE_{OUT} were shifted to zero by a constant value for better comparison; d) The actual sensor response measured at t_{meas} for various K^+ concentrations in a CaCl_2 background compared to the ISM potential measured using a conventional potentiometric measurement (dotted) at the first day (squares) and after three months (triangles). All measurements were carried out on the same device. In order to compare the potentials of the potentiometric measurements to the dynamic measurements, they were both shifted by the same constant value.

Ion selective electrodes on paper

Besides the presentation of the generalized concept, the aim of this work is also to present a fully functional low cost disposable sensor platform. For that reason two SC-ISEs were fabricated on a paper sheet by simplest means. The SC-ISE consists of a ISM which is bonded onto a PEDOT:PSS layer which was drop casted on a paper sheet. The PEDOT:PSS layer serves as an ion to electron transducer at the ISM interface and as an electrode at the same time. Based on the results obtained with the conventional setup, in order to avoid backside depletion, ISE_{OUT} was one and a half times larger than ISE_{IN} .

The SC-ISE requires ca. 15 measurement cycles to obtain a steady state response curve. Detailed stability and conditioning investigations can be found in the SUI (S4). Similar to the previously presented figure 4, figure 5a and b show the response curves of ISE_{IN} and ISE_{OUT} recorded at concentrations of 0.1 mM, 1 mM and 10 mM K^+ in a $CaCl_2$ and Na_2SO_4 background after the conditioning protocol was carried out.

Compared to the curves obtained with the conventional setup, the potential of ISE_{IN} significantly increases with time. This can be ascribed to the reduction of the conducting $PEDOT^+$ to isolating $PEDOT^0$ at the backside of the ISM.^{37,38} The amount of $PEDOT^+$, which gets reduced and consequently also the conductivity change, is defined through the current. As the current is kept constant, the dynamic potential change over PEDOT:PSS is not changed between measurements and just results in an offset. Disregarding this increasing potential, the curves are qualitatively similar to the ones obtained with the conventional setup. Accordingly, two potential jumps (1' and 2' in figure 5 a) are found. The potential jump at point 1' which is caused by the depletion of K^+ within the sample, is responsible for the measurement signal. One can clearly see the shift of the transition time to larger times upon increasing the K^+ concentration from 0.07 mM to 0.15 mM. Again at high K^+ concentrations (10 mM) the typical ionophore depletion is observable (at point 2'). Note that due to the higher current density the transition times are shifted to smaller values compared to the conventional setup. In contrast the response curves of SC- ISE_{out} are different. The response curve of the SC- ISE_{out} is characteristic to a membrane which is immediately depleted on the backside and thus on the PEDOT:PSS side. The depletion of LK^+ at the sample-side of ISE_{OUT} (point 3' in figure 5 b), which determines the maximum pulse time, is not as significant as observed with the conventional setup but still visible in the Na_2SO_4 background electrolyte.

To measure the concentration it is not necessary to record the whole response curve. Recording the potential at a certain time t_{meas} below t_{max} is sufficient. Figure 5 c shows the response of ISE_{IN} and ISE_{OUT} recorded at a measurement time of 1.8 s in a 10 mM Na_2SO_4 , a 10 mM $CaCl_2$ and a 10 mM citric acid (H^+) background. The response of ISE_{OUT} does not depend on the type of background electrolyte. Hence, ISE_{OUT} indeed provides a true reference potential during the current pulse. The response of ISE_{IN} exhibits a very high sensitivity within a narrow

concentration range. The response remains unchanged if there are no highly interfering ions within the background electrolyte (e.g. H^+ , Ca^{2+}). If highly interfering ions are present, the response is severely lowered. However, this is a general issue of flash-chronopotentiometry and can be avoided if a membrane with a higher selectivity is used.

Figure 5 d shows the actual response of the sensor for K^+ concentrations ranging from 0.1 mM to 10 mM recorded in a $CaCl_2$ background at a measurement time of 1.8 s compared to the potentiometric response which was measured before the dynamic measurements were carried out. The dynamic response shows a step drop at concentrations between $10^{-3.6}$ M and 10^{-4} M. Within this concentration range the sensitivity is increased by a factor ~ 20 compared to a potentiometric measurement (400 mV instead of 20 mV). The dynamic response remained stable, even after a period of 3 months and 120 measurements, whereas the potentiometric response exhibited a significant drift. This stability is caused by the two identical ISEs which exhibit the same potential drift. For that reason the net potential between the ISEs remains approximately zero. Consequently, the response is not influenced by mutual potential drifts of both ISMs as they cancel out.

Conclusion & Outlook

In conclusion we have presented an ion sensing platform based on two solid contact ISEs (SC-ISEs) which were fabricated on a paper sheet, by simplest means, using PEDOT:PSS and Parafilm M[®] for sealing. This concept proved to be very promising. The sensor exhibits the same characteristics as a conventional flash-chronopotentiometry setup consisting of a single ISE containing an inner filling solution and a reference electrode. Importantly, it is all-organic, solid state, does not require a reference electrode and is furthermore very simple to fabricate. Using this setup a 20 fold sensitivity enhancement compared to a potentiometric measurement was achieved. Furthermore, due to the ISEs operated in series, potential drifts of the membranes cancel out and the response of this sensor turned out to be stable for at least 3 months and 120 measurements. The response is clearly well suited for cheap disposable threshold ion sensors under conditions with physiological backgrounds. The K^+ sensitive membrane served as a model and simply by exchanging the ionophore sensitivities toward other ions can be achieved. Thus, this concept can be extended to all sorts of analytical applications.

Acknowledgements

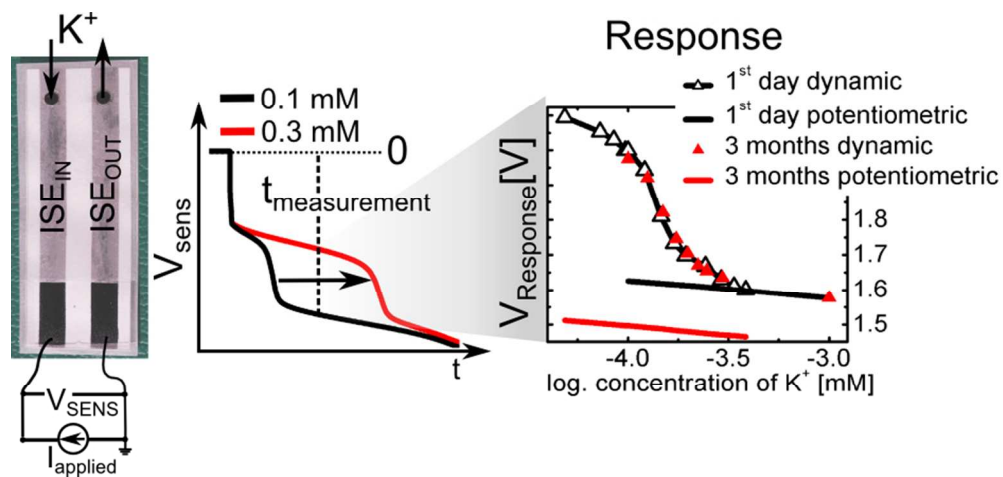
For financial support the Styrian Government (project BioOFET 2) is acknowledged.

Notes and references

^a NanoTecCenter Weiz Forschungsgesellschaft m.b.H., Franz-Pichler-Straße 32, A-8160 Weiz, Austria.

^b Institute of Solid State Physics, Graz University of Technology, Petersgasse 16, A-8010 Graz, Austria

- Electronic Supplementary Information (ESI) available See DOI: 10.1039/b000000x
- ¹ M. Tudorache and C. Bala, *Anal. Bioanal. Chem.* **388**, 565 (2007).
- ² C. Jimenez-Jorquera, J. Orozco, and A. Baldi, *Sensors* **10**, 61 (2010).
- ³ G. Hanrahan, D.G. Patil, and J. Wang, *J. Environ. Monit.* **6**, 657 (2004).
- ⁴ R. De Marco, G. Clarke, and B. Pejic, *Electroanalysis* **19**, 1987 (2007).
- ⁵ G. Crespo and E. Bakker, *RSC Adv.* **3**, 25461 (2013).
- ⁶ Y. Wang, H. Xu, J. Zhang, and G. Li, *Sensors* **8**, 2043 (2008).
- ⁷ J. Bobacka, A. Ivaska, and A. Lewenstam, *Chem. Rev.* **108**, 329 (2008).
- ⁸ E. Bakker, E. Pretsch, and P. Bühlmann, *Anal. Chem.* **72**, 1127 (2000).
- ⁹ A. Ceresa, A. Radu, S. Peper, E. Bakker, and E. Pretsch, *Anal. Chem.* **74**, 4027 (2002).
- ¹⁰ T. Sokalski, A. Ceresa, T. Zwickl, and E. Pretsch, *J. Am. Chem. Soc.* **119**, 11347 (1997).
- ¹¹ A. Malon, T. Vigassy, E. Bakker, and E. Pretsch, *J. Am. Chem. Soc.* **128**, 8154 (2006).
- ¹² G. Lisak, T. Sokalski, J. Bobacka, L. Harju, and A. Lewenstam, *Talanta* **83**, 436 (2010).
- ¹³ X.-G. Li, H. Feng, M.-R. Huang, G.-L. Gu, and M.G. Moloney, *Anal. Chem.* **84**, 134 (2012).
- ¹⁴ A. Radu, S. Peper, C. Gonczy, W. Runde, and D. Diamond, *Electroanalysis* **18**, 1379 (2006).
- ¹⁵ J. Kofler, K. Schmoltner, A. Klug, and E.J.W. List-Kratochvil, *Appl. Phys. Lett.* **193305** (2014).
- ¹⁶ K. Schmoltner, J. Kofler, A. Klug, and E.J.W. List-Kratochvil, *Adv. Mater.* **25**, 6895 (2013).
- ¹⁷ U. Mattinen, J. Bobacka, and A. Lewenstam, *Electroanalysis* **21**, 1955 (2009).
- ¹⁸ Y. Abbas, D. Balthazar de Graaf, W. Olthuis, and A. van den Berg, *Anal. Chim. Acta* **821**, 81 (2014).
- ¹⁹ W. Vonau, W. Oelßner, U. Guth, and J. Henze, *Sensors Actuators B Chem.* **144**, 368 (2010).
- ²⁰ S. Anastasova-Ivanova, U. Mattinen, A. Radu, J. Bobacka, A. Lewenstam, J. Migdalski, M. Danielewski, and D. Diamond, *Sensors Actuators B Chem.* **146**, 199 (2010).
- ²¹ T. Kakiuchi, T. Yoshimatsu, and N. Nishi, *Anal. Chem.* **79**, 7187 (2007).
- ²² T. Blaz, J. Migdalski, and A. Lewenstam, *Analyst* **130**, 637 (2005).
- ²³ A. Kisiel, H. Marcisz, A. Michalska, and K. Maksymiuk, *Analyst* **130**, 1655 (2005).
- ²⁴ H. Xu, Y. Pan, Y. Wang, G. Li, Y. Chen, and Y. Ye, *Meas. Sci. Technol.* **23**, 125101 (2012).
- ²⁵ S. Makarychev-Mikhailov, A. Shvarev, and E. Bakker, *J. Am. Chem. Soc.* **126**, 10548 (2004).
- ²⁶ M. Ghahraman Afshar, G.A. Crespo, and E. Bakker, *Anal. Chem.* **84**, 8813 (2012).
- ²⁷ S. Makarychev-Mikhailov, A. Shvarev, and E. Bakker, *Anal. Chem.* **78**, 2744 (2006).
- ²⁸ R. Ishimatsu, A. Izadyar, B. Kabagambe, Y. Kim, J. Kim, and S. Amemiya, *J. Am. Chem. Soc.* **133**, 16300 (2011).
- ²⁹ A. Shvarev and E. Bakker, *Anal. Chem.* **75**, 4541 (2003).
- ³⁰ A. Shvarev and E. Bakker, *Talanta* **63**, 195 (2004).
- ³¹ B. Gryszakowski, A. Lewenstam, and M. Danielewski, *Diffus. Fundam.* **8**, 1 (2008).
- ³² T. Sokalski, P. Lingenfelter, and A. Lewenstam, *J. Phys. Chem. B* **107**, 2443 (2003).
- ³³ J.M. Zook, S. Bodor, R.E. Gyurcsányi, and E. Lindner, *J. Electroanal. Chem.* **638**, 254 (2010).
- ³⁴ J.M. Zook, R.P. Buck, R.E. Gyurcsányi, and E. Lindner, *Electroanalysis* **20**, 259 (2008).
- ³⁵ E. Bakker and a. J. Meir, *SIAM Rev.* **45**, 327 (2003).
- ³⁶ J.J. Jasielec, R. Filipek, K. Szyszkiewicz, J. Fausek, M. Danielewski, and a. Lewenstam, *Comput. Mater. Sci.* **63**, 75 (2012).
- ³⁷ H.-S. Park, S.-J. Ko, J.-S. Park, J.Y. Kim, and H.-K. Song, *Sci. Rep.* **3**, 2454 (2013).
- ³⁸ G. a. Crespo and E. Bakker, *RSC Adv.* **3**, 25461 (2013).



We present a reference-electrode free, all organic K⁺ sensitive ion sensing platform fabricated by simplest means on a plain sheet of paper.
80x37mm (300 x 300 DPI)